

Surface Modification of Carbon-Based Nanomaterials for Polymer Nanocomposites

Manoj Karakoti¹, Sandeep¹, Sunil Dhali¹, Sravendra Rana²,
Sanka Rama V. Siva Prasanna², S.P.S. Mehta¹, Nanda G. Sahoo¹

¹KUMAUN UNIVERSITY, NAINITAL, UTTARAKHAND, INDIA ²UNIVERSITY OF PETROLEUM
AND ENERGY STUDIES (UPES), DEHRADUN, UTTARAKHAND, INDIA

2.1 Introduction

In the past decade, advancements in nanoscience and nanotechnology have been motivating the scientific community toward the discovery of new materials including carbon nanostructures such as graphene, CNTs, and fullerenes. Due to their extraordinary properties such as excellent mechanical strength, superior electrical conductivity, and magnetic properties, carbon nanostructures have been considered as one of the most promising reinforcement agents useful for enhancing the properties of polymer composites. The carbon nanomaterials are classified according to their dimensionality into the three classes. The first material of this class is zero-dimensional (0-D) buckminsterfullerene (C₆₀), a Nobel Prize-winning discovery by Kroto et al. in 1985 [1] that created a new division of carbon chemistry [2,3]. Fullerene consists of 12 pentagons and 20 hexagons rings and has a soccer ball-like structure with 7.1 Å and an approximately 10 Å center-to-center distance between neighboring molecules in a single crystal [4]. Due to their exceptional molecular structures, fullerenes and their derivatives have shown interesting photonic, electronic, superconducting, magnetic, and biomedical properties [4,5]. The succeeding discovery of one-dimensional (1-D) CNTs by Iijima [6] was a revolutionary change in the branch of materials science and nanotechnology [7,8]. These cylindrical-shaped nanotubes consist of hexagonal carbon rings arranged in a concentric style with both ends of the carbon tube often capped by fullerene-like structures containing pentagons. At the molecular level, CNTs can be viewed as a small strip of graphene sheet rolled up into a tube-like structure in the nanoscale range called a single-walled carbon nanotube (SWNT). There may be additional graphene sheets following the coaxial tubes around the SWNT core to form a multiwalled carbon nanotube (MWNT) [5,6,9]. CNTs have gained considerable attention as a new and valuable member of the carbon family with their exceptional novel attributes, such as electronic, optoelectronic, and electrochemical properties. Because of these

interesting properties CNTs are attractive for a variety of potential applications, such as sensors [10], hydrogen-storage systems [11], piezoelectric and thermoelectric energy-harvesting devices [12,13], organic photovoltaic cells [14], fuel cells [15,16], batteries [17], and supercapacitors [18].

Graphene was firstly discovered in 2004 by Novoselov and his group by simple mechanical exfoliation of graphite, using a scotch tape method, into gradually thinner pieces until individual atomic planes were reached [19]. The graphene, two-dimensional (2-D) one-atom-thick planner sheet of sp^2 bonded carbon atom was arranged in a honeycomb structure. It shows superb properties as well as having a large surface area, graphene nanosheets (GNs) with a 2-D carbon nanostructure have been studied under a new class of carbon chemistry for their potential applications in various fields such as sensors, actuators, solar cells, field-emission devices, field-effect transistors, supercapacitors, and batteries [20–27].

These aforementioned classes of carbon nanomaterials are well-known for their extraordinary properties. Due to these properties, nanomaterials are used as a filler for polymer nanocomposites. For the synthesis of nanocomposites these carbon nanomaterials are used as a filler for the polymer nanocomposites in polymer matrix. Nanofilled polymeric matrices have produced amazing mechanical, electrical, and thermal properties. A broad range of fillers are used in reinforcing polymer matrixes, however, this chapter focuses on the processing of carbon nanotube and graphene as potential nanofillers to form nanocomposites as well as the various surface modification techniques for carbon nanomaterials through noncovalent and covalent functionalization. The high degree of reinforcement is observed when the filler range is 100 nm and below [28]. Thus the size and other properties, including high mechanical strength and high aspect ratio of carbonaceous nanofillers, such as nanotubes and graphene, have emerged their use as potential nanofillers for polymer nanocomposites. However, problems arise with the agglomeration and solubility of carbonaceous materials in aqueous and organic solvents as well as an increase in the interaction with the polymer matrix. To minimize this problem, surface modification of carbon nanomaterials for the synthesis of polymer nanocomposites and enhancing their properties in various fields is carried out, as summarized in Fig. 2-1.

2.2 Surface Modification of Carbon Nanomaterials for Polymer Nanocomposites

Since carbon nanomaterials (graphene and CNTs) usually agglomerate due to van der Waals force, dispersion and alignment of these materials in a polymer matrix is extremely difficult. Thus, it is a challenge to develop high-performance polymer–graphene/CNT-based composites to achieve better dispersion and alignment and strong interfacial interactions, for better load transfer across the CNT/graphene–polymer matrix interface. The functionalization of these materials is an effective way to avoid the aggregation of CNTs and graphene, which helps them to better disperse and stabilize within a polymer matrix. There are two main

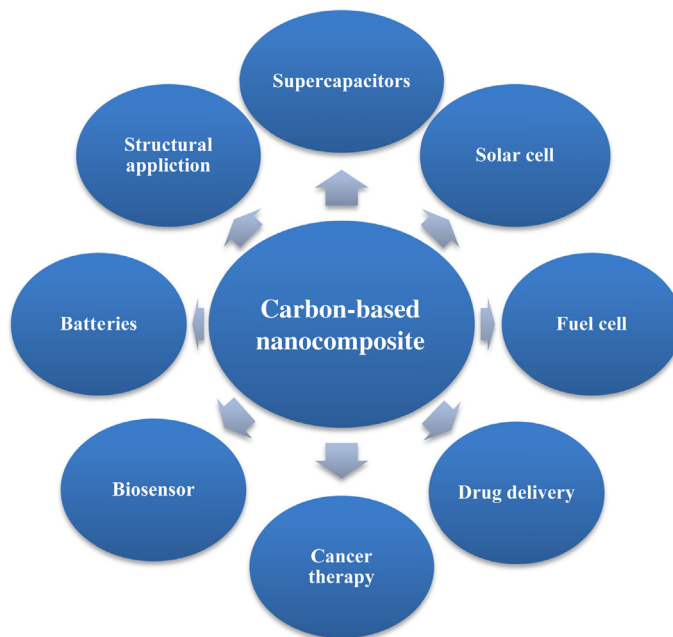


FIGURE 2-1 Application of carbon-based nanocomposites in various fields.

approaches for the functionalization of graphene/CNTs, these functionalization methods are summarized here:

1. Surface modification via noncovalent functionalization;
2. Surface modification via covalent functionalization.

2.2.1 Surface Modification Via Noncovalent Functionalization

Carbon nanomaterials have attracted much attention on account of their potential to be transformed into new materials that can be employed to address a wide range of applications. Due to the insolubility of the carbon nanomaterials in most solvents their real-life applications are restricted. For better solubility of carbon nanomaterials, their surface is modified by noncovalent functionalization as well as to preserve the desired properties while remarkably improving their solubility. This section describes the recent advances in the design, synthesis, and new methods for the noncovalent functionalization of carbon nanomaterials which promises a new generation of carbon nanomaterial for hybrid-based integrated multifunctional sensors and devices, an outcome which is essential for the development of carbon nanomaterials chemistry that interfaces with different fields of science. Noncovalent functionalization of carbon nanomaterials through aromatic compounds, surfactants, biomolecules, and polymers are connected by π - π stacking or hydrophobic interactions, electrostatic interaction, and hydrogen bonding. In these approaches, noncovalent

modifications of carbon nanomaterials does not compromise their physical properties and conserves their desired properties, while improving their solubility quite remarkably.

2.2.1.1 Surface Modification of Graphene Via Noncovalent Functionalization

Surface modification of graphene is significant because of π - π stacking and van der Waals force that exist between the graphene sheet consequences, reside in multilayer due to this impermanent interaction of graphene sheet becomes hydrophobic in nature and cannot be dissolved in aqueous and organic solvents. To overcome this problem it is required to increase its solubility in common solvents, and thereby avoid stacking between the graphene layers through the noncovalent functionalization with different surface-modifying agents [29].

Liu and coworkers [30] synthesized a composite material of graphene-PNIPAAm, by pyrene-terminated reversible addition fragmentation chain transfer (RAFT) of PNIPAAm (10 mg, 1.0×10^{-6} mol) dissolved in water and then added it to an aqueous solution of graphene. After that the resulting mixture was sonicated in an ice bath for 20 min, it was centrifuged at 14,000 rpm for removal of water from the mixture. After removing the water, the resulting composite material of graphene-PNIPAAm was redispersed in water under mild sonication and then centrifuged. The AFM study indicates a thickness of 1.4 nm through the line profile (Fig. 2-2A) [31-33]. Pyrene-functionalized polymer attached both sides of the graphene sheet through π - π stacking to form a sandwich-like structure. The thickness of the graphene-PNIPAAm sandwich was 5.0 nm, as revealed by atomic force microscopy analysis (Fig. 2-2B). The thickness of the graphene-polymer composite is much less than the value predicted based on an assumption that all the polymer chains attached are vertically stretched to the graphene basal plane. The result related to the conformation adopt by the flexible polymer chain is entropically favored on the graphene sheet through noncovalent functionalization. Further analysis of the polymer composite based on the graphene-PNIPAAm by scanning electron microscopy is shown in Fig. 2-2C. Some samples of polymer composite are aggregated because these samples are prepared in concentrated composite aqueous solution, as can be clearly observed through the SEM images. In other samples of this polymer composite in spin coating dilution of graphene-PNIPAAm over the flat silicon substrate, and observed from the SEM images separate and flat sheet of graphene-PNIPAAm (Fig. 2-2D).

Qin et al. [34] synthesized nanocomposite materials of polyimide/graphene via an in situ polymerization approach. Here the noncovalent functionalization of graphene by using aromatic molecules is valuable over a chemical modification method because it does not reduce the structure of graphene [29]. It has also been reported that polyaniline and its oligomers exhibited a particular capability for the dispersion of graphene, in various solvents or in a polymer matrix [35,36]. The approach from his group was an amine-aniline trimer (AT) used as a dispersant of graphene in a polyimide (PI) matrix homogeneously along the reactive component for polyimide (PI) and form graphene/PI interface composites, as shown in Fig. 2-3. In the first step, in the presence of AT, a few atom thick graphene layers are exfoliated from pristine graphene in dimethylacetamide (DMAc). Then in the second step, using

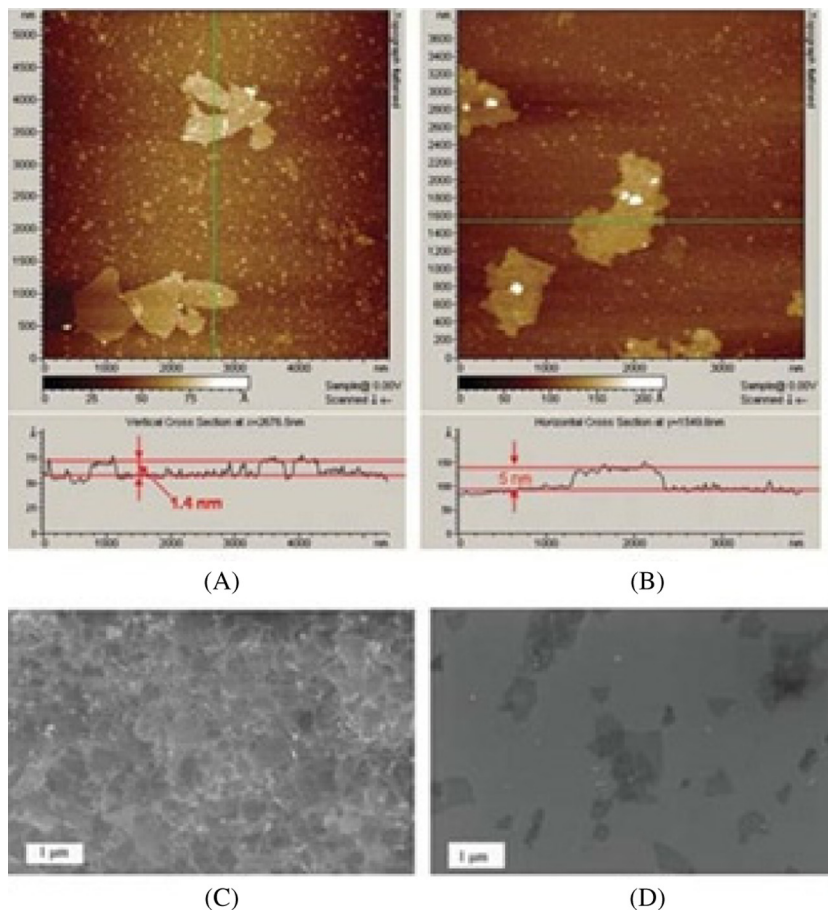


FIGURE 2-2 Images from before and after modification of graphene with pyrene-functional PNIPAAm through $\pi - \pi$ stacking: (A) unmodified AFM image of graphene; (B) AFM image of composite by graphene–PNIPAAm; (C) high-resolution SEM images show the aggregation of graphene–PNIPAAm composite; and (D) high-resolution SEM images show the dispersion of graphene–polyNIPAAm composite prepared by spin-coating on a silicon substrate [30].

various amounts of AT-functionalized graphene nanosheet and the suspension of poly(amic acid) (PAA)/graphene is prepared via in situ polymerization of pyromellitic dianhydride (PMDA), 4,4-oxydianiline (ODA) under N_2 atmosphere at room temperature. In the third and final step, at an elevated temperature thermal imidization of PPA/graphene hybrid gives polyimide/graphene nanocomposites.

In UV-vis spectroscopy, AT gives two characteristic absorption peaks of benzenoid and quinoid at 336 nm and 582 nm, respectively, in DMAc. Similarly, AT/graphene exhibited two absorption peaks, but due to $\pi - \pi^*$ transition of benzenoid was blue shift from 336 nm for AT and 328 for AT/graphene, i.e., peaks shifted by 8 nm, which clearly gives the indication of $\pi - \pi^*$ transition between AT and graphene. Raman spectra of graphene give the

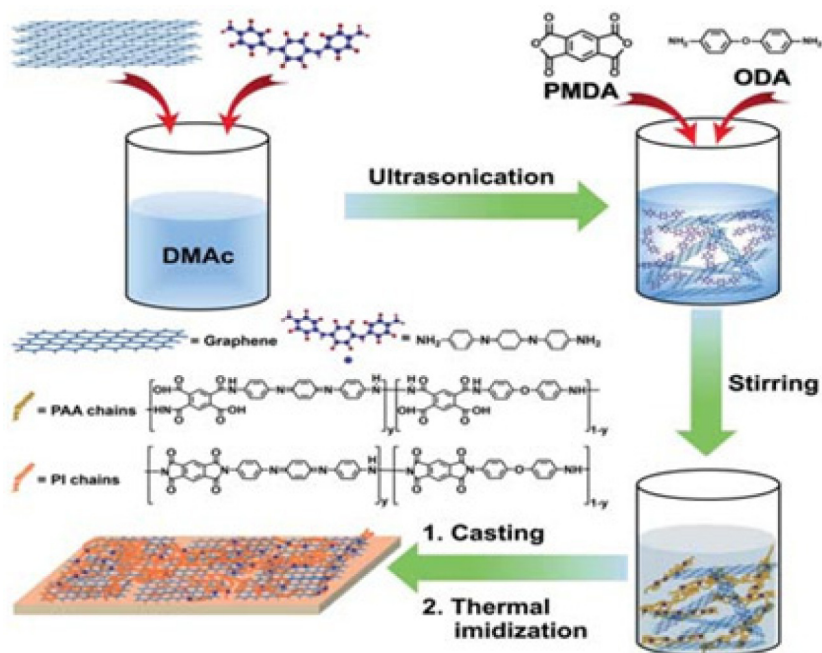


FIGURE 2-3 Schematic representation for the synthesis of PI/G composite films via in situ polymerization [34].

characteristics peaks at 1582 cm^{-1} and 1336 cm^{-1} for G band and D bands, respectively. On the other side AT gives peaks at 1346 cm^{-1} , 1499 cm^{-1} , and 1577 cm^{-1} for C–N stretching, phenazine absorptions at and C=C stretching of the quinonoid ring respectively, which reveals the π – π interaction between graphene and AT.

2.2.1.2 Surface Modification of Carbon Nanotubes via Noncovalent Functionalization

Carbon nanomaterials are poorly soluble in most organic solvents due to their tendency to become entangled and form 3-D networks through determined van der Waals interactions. Therefore, noncovalent functionalization becomes a more attractive solution for various groups attached onto the CNT surfaces without affecting the conjugated π system and also increasing the solubility in aqueous and organic solvents [37]. The noncovalent approaches are based on interactions of the hydrophobic part of the adsorbed molecules with nanotubes sidewalls through van der Waals, π – π , CH– π , and other interactions, resulting in aqueous solubility by the hydrophilic part of surface-modifying agents [38]. The charge on the nanotube surface by adsorbed ionic molecules additionally prevents nanotube aggregation by the coulombic repulsion forces between modified CNTs. In the last few years, the noncovalent treatment of CNTs with surfactants and polymers has been widely used in the preparation of both aqueous and organic solutions to obtain a high weight fraction of individually dispersed nanotubes. Polymers favor CNT dispersion in polar solvent, due to wrapping of polymer or

block copolymer in the CNT surface through a hydrophobic part and exposing their polar domain towards the polar solvent [39]. Luo and coworkers [40] synthesized a pyrene-containing polymer for side wall functionalization of multiwalled carbon nanotubes through π - π stacking. After the functionalization of multiwalled CNTs by pyrene increased the dispersion in good solvent for PMMA and the interaction between MWCNTs/PMMA also increases the load transfer from polymer to CNT.

Anionic, cationic, and nonionic surfactants also favor the dispersion of CNTs in water. To avoid the aggregation of CNTs anionic surfactants such as sodium dodecylsulfate (SDS) [41–43] and sodium dodecylbenzene [44,45] are used. The interaction between CNTs and surfactant depends upon the properties of the surfactant such as alkyl chain, head group size, and charge towards the CNT [46]. Surfactants such as NaDDBS and Triton-X100 have far better interaction due to benzene ring with CNTs than SDS. Certainly, π - π interactions of benzene with the outer surface of CNTs enhanced the binding and covered the surface of CNTs by surfactant appreciably [47], due to having a head group and slightly longer alkyl chain in NaDDBS they dispersed better than Triton-X 100. Sgobba and coworker published a report on the use of carbon nanotubes for fabricating flexible, transparent, large-scale organic photovoltaic devices [48]. The two main promising routes were use of CNTs in photovoltaic devices as photoactive materials and semitransparent conducting materials for electrodes preparation. The Zaumseil research group synthesized a composite material of poly(9,9-dioctylfluorene) (F8) or poly(9,9-dioctylfluorene-cobenzothiadiazole) (F8BT) with SWCNTs [49]. For the selection of a new polymer for these composite materials some parameters are considered such as solvent type, polymer molecular weight, concentration, and viscosity in hybrids for dispersion of SWCNTs in a polymer matrix. After the investigation of these composite materials it was found that viscosity is a prominent factor for the dispersion of SWCNTs. The same group also studied how a small amount of SWCNTs dispersed in F8BT and F8 polymer matrix influence device characteristics of bottom/top gate ambipolar light-emitting field-effect transistors [50]. The final results showed that reduced contact resistance and lesser threshold voltages show the way to larger ambipolar currents and consequently brighter light emission. A systematic representation of how transistors are prepared from dispersion of SWCNTs in conjugated polymer is given in Fig. 2-4.

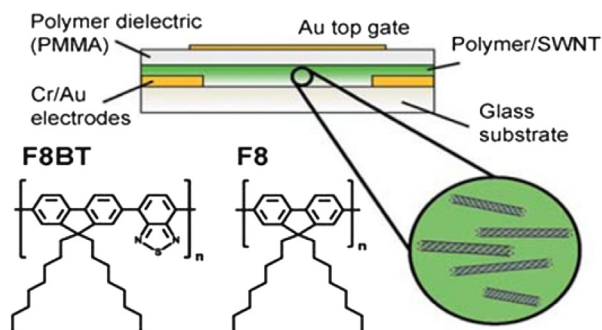


FIGURE 2-4 Schematic representation of bottom contact/top gate polymer field-effect transistor with CNTs dispersed in the semiconducting polymers F8BT and F8 [50].

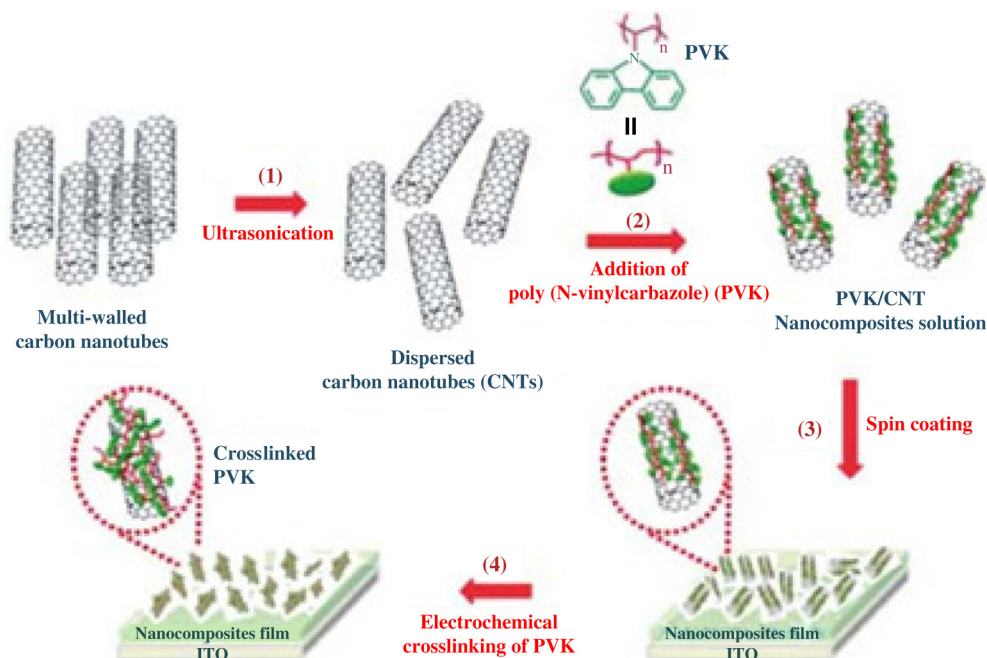


FIGURE 2-5 Illustration for the synthesis of PVK–MWCNT nanocomposites through MWNT dispersion in a mixed solvent, spin-coating and electrodeposition [51].

Cui et al. [51] employed easy methods for the preparation of composite as well as fabrication of a nanocomposite film of poly(N-vinyl carbazole) (PVK) and MWCNTs. For better dispersion and to avoid the aggregation of MWCNTs in the PVK polymer matrix, the solution was prepared through sonication. The major achievement of this process was that the composite solution was stable for a long time without any precipitation of MWCNTs (Fig. 2-5).

The surface modification of carbon nanotubes through ionic interaction between CNTs and polyelectrolytes has also been studied. The polyelectrolyte provides positive and negative charge on the surface of CNTs, which gave the opportunity for the preparation of a CNT-based hybrid nanostructure. Rouse et al. investigated the method for preparation of uniform polymer/SWCNT films through absorption of poly(diallyldimethylammonium chloride) (PDDA) chise by carbon nanotube with high concentration on substrate [52]. Another group used the same electrolyte for surface modification of CNTs in an oxygen reduction catalyst for fuel cell and made them metal free-catalyst with performance up to the Pt catalyst [53].

2.2.2 Surface Modification Via Covalent Functionalization

In the case of covalent functionalization, the translational symmetry of CNTs and graphene is disrupted by changing sp^2 carbon atoms to sp^3 carbon atoms, and the properties of

nanofillers, such as electronic and transport are influenced. In covalent functionalization, graphene and CNTs are linked with a functional unit through covalent linkage. There are several methods for covalent functionalization of these carbon nanomaterials.

2.2.2.1 Functionalization of CNTs and Graphene Using Click Chemistry

The introduction of a highly regioselective CuI-catalyzed alkyne–azide cycloaddition reaction (click chemistry) initiated a golden period for cycloaddition reactions, which have found multiple applications in areas including biomedical science, organic synthesis, and material science [54]. Due to its high regioselectivity and yield, easy reaction conditions, good reliability, and tolerance to a wide range of functional groups, the CuI-catalyzed cycloaddition reaction has played an important role in the synthesis of small molecules, dendrimers, and biologically active macromolecular structures [55].

2.2.2.1.1 FUNCTIONALIZATION OF CNTS USING CLICK CHEMISTRY

A first report onto the CNT functionalization using the Cu(I)-catalyzed Huisgen [3 + 2] cycloaddition reaction was published by Li et al. [56]. A high degree of functionalization was achieved by the coupling of the azide group terminated polystyrene and alkyne-functionalized SWCNT, where polystyrene was synthesized using ATRP and further transformed to azide-terminated polystyrene. This reaction was extremely efficient at low reaction temperatures and with a short reaction time, producing organo-soluble polymer nanotube conjugates with a high graft density and controlled polymer molecular weight. The polystyrene-functionalized SWCNTs were found to be soluble in an organic medium and completely insoluble in the aqueous layer. However, when the authors achieved the sulfonation of the grafted polystyrene, the sample was found to be completely insoluble in the organic medium and fully soluble in the aqueous medium [57]. Click coupling was also applied for the successful grafting of polyurethane onto the CNT surface. Rana et al. successfully synthesized the polyurethane-grafted SWCNTs by coupling of alkyne moiety decorated SWCNTs with the azide moiety containing polyurethane using click chemistry [58]. First, ROP was applied to synthesize the azide moiety containing poly(ϵ -caprolactone)diol (PCL-diol) and further treated with 4,4'-methylenebis(phenylisocyanate) (MDI) to prepare the azide moiety decorated polyurethane. Due to chemical bond formation between polyurethane and SWCNT at some intervals, individual SWCNTs were observed.

Click reaction was also applied to prepare the nanocomposites based on hyper-branched polymer–CNT materials. Yadav et al. [59] prepared the nanocomposites of MWCNTs and hyper-branched polyurethane (HBPU) via a click chemistry reaction. They prepared the various compositions of HBPU-functionalized MWCNTs from the reactions of azide moiety-containing HBPU with alkyne-functionalized MWCNTs. The functionalized MWCNTs exhibited excellent dispersion in the HBPU matrix, and, as a result, superior mechanical properties were achieved for the composites. The prepared HBPU–CNT nanocomposites also showed good biocompatibility properties. Click chemistry along with ROP were achieved on the CNT surfaces [60], where hydroxyl-groups decorated MWCNTs were used as coiniciators to polymerize PCL and poly(α -chloro- ϵ -caprolactone) by surface-initiated ROP, where pendent

chlorides were converted into azides by reaction with sodium azides. Finally, various types of terminal alkynes were reacted with pendent azides by click reaction. The MWCNT-g-PCLs and MWCNT-g-(P α N $_3$ CL-g-alkyne)s were well dispersed in the organic solvent. The observed average thickness of the wrapped polymer layer was approximately 8–10 nm for MWCNT-g-PCL and 3 nm for MWCNT-g-(P α N $_3$ CL-g-PBA). Poly(styrene-*b*-(ethylene-co-butylene)-*b*-styrene) triblock copolymer (SEBS) functionalized MWCNTs were prepared using click chemistry reaction [61]. The reaction between azide moieties containing SEBS on styrene with alkyne in wrought MWCNTs gives a different composition of SEBS-functionalized MWCNTs. The functionalized MWCNTs showed excellent dispersion in the SEBS matrix, and, as a result, extremely improved mechanical properties and high dielectric constant, as well as enhanced thermal stability, were observed. The click-coupled bonding of MWCNTs with SEBS was very effective for controlling the material properties and achieving high-performance materials.

Regarding the application of CNTs for the promising carriers meant for genetic material, ammonium and guanidinium dendron decorated carbon nanotubes by amidation and click chemistry were prepared [62]. A series of MWCNT conjugates were described functionalized with different dendrons bearing charges at their termini (i.e., ammonium or guanidinium groups). The demonstration of the cell uptake capacity, the low cytotoxicity, and the ability of these cationic conjugates to silence cytotoxic genes suggests them to be promising carriers for genetic material. Coating of CNTs with magnetic nanoparticles (NPs) imparts novel magnetic, optical, and thermal properties with potential applications in the biomedical domain. MWCNTs were decorated with iron oxide super paramagnetic NPs [63]. Two different approaches have been investigated based on ligand exchange or click chemistry. The presence of the NPs on the nanotube surface allows conferring of magnetic properties to CNTs. The authors evaluated the potential of the NP/CNT hybrids as a contrast agent for magnetic resonance imaging (MRI) and their interactions with cells. The NP/CNTs can be manipulated by a remote magnetic field with enhanced contrast in MRI. They are internalized into tumor cells without showing cytotoxicity. The labeled cells can be magnetically manipulated as they display magnetic mobility and are detected at a single cell level through high-resolution MRI. SWCNTs were incorporated into poly(vinyl alcohol) hydrogels by click chemistry. This efficient and modular reaction allowed preparation of hydrogels with crosslinker molecules of various properties, such as hydrophilic or hydrophobic character [64]. Control of crosslinking density and mole transport inside the hydrogels was demonstrated by measuring degrees of swelling and electrochemical diffusion coefficient of an ionic solute. Incorporation of SWCNTs into the hydrogels aided the growth of poly(3,4-ethylenedioxythiophene) (PEDOT), presumably due to the enhancement of electrochemical conditions.

Nicolas et al. analyzed the impact of CNTs functionalization on their biocompatibility via the culture of stem cell [65]. Rana et al. demonstrated a straight-forward click-chemistry-based approach for the functionalization of SWCNTs with oligo-lysine dendrons. Peptide dendron functionalized nanotubes showed significantly increased biocompatibility in rat mesenchymal stem cell culture. MWCNTs were covalently functionalized with PCL using click chemistry [66]. Chlorine moiety containing PCL was synthesized by

the copolymerization of α -chloro- ϵ -caprolactone with ϵ -caprolactone monomer using ROP, and further converted to azide moiety-containing PCL. The alkyne functionalized MWCNTs were prepared with the treatment of p-amino propargyl ether using a solvent-free diazotization procedure. The covalent functionalization of alkyne-derived MWCNTs with azide moiety-containing PCL was accomplished using click chemistry. Azides derived from different amino acids were also coupled with alkyne-functionalized SWCNTs through the 1,2,3-triazole ring using the Cu(I)-catalyzed Huisgen [3 + 2] cycloaddition reaction between alkynes and an excess of azides [67]. As a result, a high degree of functionality on SWCNTs was obtained. The functional route would be a very efficient tool for the functionalization of SWCNTs with a variety of biomolecules such as peptides and polysaccharides. Purified SWCNTs were reacted with p-(2-propynyloxy)-benzenamine in o-dichlorobenzene using a diazotization-coupling procedure to produce alkyne-functionalized SWCNTs and further treated with azide-functionalized cyclodextrin via Cu(I)-catalyzed Huisgen [3 + 2] cycloaddition [68]. The β -cyclodextrin functionalized SWCNTs showed good solubility in water, enhancing their biological importance for drug delivery applications.

Due to their synergetic properties, CNT and metal particle-based hybrid nanomaterials play important roles in several application areas, including electronic, optical, catalytic, and magnetic applications [69–71]. Voggu et al. have synthesized a novel material by functionalization of SWCNTs with gold nanocrystals [72]. They achieved SWCNT functionalization with amidobutane containing a terminal azido group and further treated with Au nanocrystals capped with the hex-5-yne-1-thiol. This reaction yielded a SWCNTAu nanomaterial, in which the gold nanocrystals decorated the SWCNTs. Nanohybrids comprising MWCNTs and Au-coated Fe nanoparticles (Fe@Au NPs) have been developed [73]. The Fe@Au NPs anchored with MWCNTs (Fe@Au/MWCNTs) were initially prepared by the interaction of azide groups decorated Fe@Au NPs and alkyne-functionalized MWCNTs via the Cu(I)-catalyzed 1,3-dipolar cycloaddition reaction. A superconducting quantum interference device (SQUID) study indicated that the nanohybrids had ferromagnetic character, which was susceptible to a rapid separation of colloidal magnetic materials under an external magnetic field. Regarding the photocatalytic application of CNT-based hybrids, the hybrid assembly composed of thin MWCNT and titanium dioxide (TiO_2) was prepared by using click chemistry [74]. TiO_2 -decorated thin MWCNT hybrids with anatase phase TiO_2 were obtained from the reaction of an azide moiety-containing TiO_2 with alkyne-functionalized MWCNTs. The nanohybrid is extremely active and lasting for photocatalytic degradation of methyl orange.

A further study was carried out by Rana et al. [75], wherein they achieved functionalization of SWCNTs by gold nanoparticles through the Huisgen cycloaddition reaction. Gold nanoparticles containing octane thiol moieties were prepared by the reduction of tetrachloroauric acid using sodium borohydride in the presence of alkanethiol. The alkyl thiol-protected gold nanoparticles were further treated with azido undecane-thiol to yield the azide-moiety containing gold nanoparticles. As a strategy for the attachment of metal nanoparticles, the 1,2,3-triazole ring was utilized as a linker between the azide-decorated nanoparticles and alkyne-functionalized SWCNTs. The covalent functionalization of MWCNTs with pyrene via Cu(I)-catalyzed azide/alkyne click (CuAAC) reactions under mild conditions

to afford the nanocomposites of pyrene-MWCNTs was reported [76]. The CuAAC reaction occurred in an efficient manner and the spacer linking MWCNTs and the photo-active molecule was well discussed. In contrast to the noncovalent functionalization of $\pi-\pi$ stacking, the nanocomposites of pyrene clicked MWCNTs showed relatively strong fluorescence and had potential applicability in photoluminescent devices as a highly sensitive and selective fluorescence turn-off sensor for Fe^{3+} .

Core-shell nanowires having MWCNT as a core and polypyrrole (PPy) as a shell were synthesized using click chemistry [77], where uniform PPy layers of 10–20 nm in thickness were formed well on the MWCNT surface. In particular, “grafting from” click coupling was more effective in obtaining uniform and stable core-shell nanowires as well as in the reaction yield, compared to “grafting to” click coupling. This is due to chemical bond formation between PPy and MWCNT in equal intervals along the longitudinal direction of the MWCNT, achieved by “grafting from” click coupling.

Campidelli et al. used the click methodology to synthesize phthalocyanine functionalized SWCNTs [78]. Photo-induced communication between the two photoactive components (i.e., SWCNT and ZnPc) was also identified. These features are helpful in incorporating the SWCNT–ZnPc hybrid in a photo electrochemical cell as a photoactive material in an ITO photo anode. The functionalization of SWCNTs with zinc porphyrins (ZnP) using click chemistry has been reported [79]. Strong electronic coupling between the photo- and electro-active constituents led to rapid excited-state deactivation of ZnP via the charge transfer to the nanotubes. Photophysical assays by means of steady-state reveal that the selective photo excitation of ZnP derivatives is followed by a rapid charge separation, namely, the formation of reduced SWCNT and oxidized ZnP.

2.2.2.1.2 FUNCTIONALIZATION OF GRAPHENE USING CLICK CHEMISTRY

A facile click chemistry methodology has been developed to immobilize well-defined polymers onto graphene sheets using click chemistry [80]. The polystyrene functionalized highly exfoliated graphene sheets were observed in different organic media, where triblock SEBS copolymer functionalized graphene oxide sheets were prepared via click chemistry [81]. For the potential applications of the block copolymer clicked GO sheets, the functionalized nanomaterials were incorporated into PS as reinforcing fillers. The SEBS-clicked GO sheet showed excellent compatibility with a PS matrix, and, as a consequence, remarkably improved mechanical properties and thermal stability of the resulting composite films was achieved.

RAFT polymerization and click chemistry approaches were applied together to achieve individually dispersed graphene nanosheets (GNs) [82]. Graphene with an alkyne core was used to synthesize the polymer-functionalized graphene using “grafting to” and “grafting from” strategies in combination with reversible chain transfer and click chemistry. The use of the “grafting to” approach allows full control over limited-length grafted polymer chains, while permitting a high grafting density to a single graphene face resulted in good solubility and processability. The “grafting from” approach offers complementary advantages, such as the grafting of high-molecular-weight polymer chains and a better coverage ratio on the graphene surface.

PLC–graphene sheet (GS) reinforcing fillers were synthesized through click coupling and demonstrate covalent functionalization graphene oxide with PLC, and afterwards PLC–graphene sheet nanofiller was integrated into shape memory polyurethane matrix by solution casting [83]. The tremendous interaction between PLC–GS nanofiller with polyurethane matrix was responsible for enhancement of thermal conductivity, mechanical properties, and thermo-responsive shape memory properties of the resulting nanocomposite film. Especially, incorporation of 2% PLC–GS nanofiller with polyurethane nanocomposite improved breaking stress, Young's modulus, elongation-at-break, and thermal stability by 109%, 158%, 28%, and 71%, respectively.

Thermotropic liquid crystalline polymer modified graphene and its reinforcement effect in the polymer matrix were analyzed, where the authors first covalently functionalized the graphene oxide with propargyl alcohol to obtain alkyne terminated graphene oxide [84]. These alkyne groups on graphene oxide sheets were further reacted with a kind of azido-functionalized liquid crystal polymer via click chemistry. The liquid crystal polymer introduced was a side-chain liquid crystal polymer-poly(2,5-bis[(4-methoxyphenyl)oxycarbonyl]styrene) (PMPCS). The prepared GO–PMPCS composite had potential applications in improving the mechanical properties of liquid crystal PMPCS matrix. The effect of the type of chemical route used to functionalize graphene with short-chain polyethylene on the final properties of graphene-based high-density polyethylene nanocomposites was also discussed. Three different click reactions, namely CuAAC, thiol-ene, and thiol-yne were discussed by Horacio et al. [85]. The nanocomposites were prepared using a method “gradient interphase.” The electrical and thermal conductivity and the mechanical properties strongly depended on the click reaction used to modify graphene, the thiol-ene reaction giving the best results. This study demonstrated that the election of the chemical strategy to provide graphene with functionalities common to the polymer matrix and the engineering of the interface was crucial to obtain nanocomposites with improved properties.

The click chemistry strategy provides a facile and general method for functionalization of graphene oxide with macromolecules and desired biomolecules [86–88]. A novel DNA-templated click chemistry strategy for homogeneous fluorescent detection of Cu^{2+} has been developed based on click ligation-dependent DNA structure switch and the selective quenching ability of the GO nanosheet [89]. The clickable duplex probe consists of two DNA strands with an alkyne and azide group, respectively, and the Cu^+ -catalyzed alkyne azide cycloaddition. CuAAC reaction can chemically ligate these two strands. The probe transfer to single-stranded DNA (ssDNA) tail caused by Cu^{2+} induced chemical ligation, whereas the duplex structure of DNA was obtained without Cu^{2+} . Therefore GO-based fluorescence detection is used for the determination of structure difference between the ssDNA and duplex structure DNA, due to greater binding capacity with ssDNA. These types of sensor are particularly for detections of Cu^{2+} with a low limit of 58 nM and a linear range of 0.1–10 mM under optimum conditions. This is a highly sensitive and selective technique for detection of Cu^{2+} due to the quenching ability of GO and the specificity of click chemistry.

CuPt-nanorod anchored GO composites using a click reaction have been demonstrated [90]. CuPt-nanorods with controlled size, aspect ratio (from 1 to 11), and uniformity have been synthesized. Their catalytic properties in the water phase are investigated using an *o*-phenylenediamine oxidation reaction. The results of this study clearly demonstrate that non-polar CuPt-nanorods immobilized on GO can function as a catalyst in an aqueous solution and that GO can be used as a catalytic nanorod support. A synthetic strategy is developed that allows for the facile functionalization of carbon nanostructures with conducting polymers [91–93], thus providing the possibility of comparing the strikingly different optical and electrochemical properties of ensembles based on the conducting polymers covalently attached to either CNT or graphene. Poly(3-hexylthiophene) (P3HT) brushes on GO sheets via a silylation reaction of the surfaces of GO sheets and a succeeding click reaction (GO(C)/P3HT composite) have been discussed [93]. Compared with pure P3HT and the blend of P3HT and GO, the GO(C)/P3HT composite showed a red-shifted optical absorption maximum because of the increased conjugation length of the grafted P3HT, which might be due to the crowding of the P3HT chains grafted on GO sheets. For comparison, P3HT chains were also grafted on GO sheets via amidation reaction of the carboxylic acid groups GO(A)/P3HT composite. However, the GO(A)/P3HT composite did not show a red shift in the UV-visible spectrum. The overall fluorescence quenching in the GO(C)/P3HT composite includes both dynamic quenching and forming a nonfluorescent ground-state complex.

Pan et al. have covalently functionalized graphene sheets with a well-defined thermo-responsive PNIPAm via the click chemistry approach [94]. The PNIPAm-grafted graphene sheets (PNIPAm-GS) consist of about 50% polymer, which endows the sheets with good solubility and stability in several solvents. Due to the contact between graphene sheets and grafted PNIPAm, the PNIPAm-GS show hydrophilic to hydrophobic phase transition at 33°C, which is comparatively lower than that of a PNIPAm homopolymer. Besides, the hydrophobic interaction between PNIPAm-GS and an aromatic drug through π – π stacking, results in PNIPAm-GS being able to load a water-insoluble anticancer drug, camptothecin, with a higher loading capacity. Based on click chemistry and RAFT, PNIPAm polymer brushes on the surfaces of reduced graphene oxide (rGO) sheets were reported [95]. rGO sheets prepared by thermal reduction were modified by diazonium salt of propargyl *p*-aminobenzoate, and alkyne-functionalized rGO sheets were obtained. RAFT chain transfer agent was grafted to the surfaces of rGO sheets by click reaction, and PNIPAm on rGO sheets was prepared by RAFT polymerization. Differential scanning calorimetry (DSC) results indicated that in aqueous solution, PNIPAm on rGO sheets presented a lower critical solution temperature at 33.2°C. Click chemistry was also applied to introduce light-responsive β -cyclodextrin (CD)-based [2] rotaxanes onto GO surfaces [96]. The [2] rotaxane-functionalized GO is more dispersible and has higher stability in aqueous solution than nonfunctionalized GO. The β -CD ring in the system can be reversibly switched between two stations by alternating irradiation with UV and visible light, controlled by the light-sensitive [2] rotaxane as an antenna on the GO surfaces. The [2] rotaxane-functionalized GO provides a light-responsive platform for manufacturing information storage and memory devices.

2.2.2.2 Functionalization of CNT and Graphene Using Block Copolymers

Poor solubility of CNTs in water and organic solvents presents a considerable challenge for their purification and applications. Macromolecules can be convenient solubilizing agents for CNTs and a structural element of composite materials for them. The microphase separation of the individual polymer components and the resulting formation of well-defined nano-sized domains provide a broad range of new materials with various properties. Block copolymers facilitated the development of innovative concepts in the fields of drug delivery, nanomedicine, organic electronics, and nanoscience [97,98]. In this chapter, we discuss selected examples of recent developments regarding CNT and graphene functionalization with block copolymers and their applications.

2.2.2.2.1 FUNCTIONALIZATION OF CNTS USING BLOCK COPOLYMERS

There are several reports on block copolymer functionalized CNTs [99–107]. Polystyrene and poly[(*tert*-butyl acrylate)-*b*-styrene] with well-defined molecular weights and polydispersities were prepared by nitroxide-mediated free-radical polymerization [99]. The homopolymers and block copolymers were used to functionalize shortened SWCNTs through a radical coupling reaction involving polymer-centered radicals generated at 125°C via loss of the stable free-radical nitroxide capping agent. The resulting polymer–SWCNT composites were found to be highly soluble in a variety of organic solvents. Jung et al. have reported the block copolymer polyurethane (PU) crosslinked CNT composites [103]. MWCNTs functionalized by chemical modification were incorporated as a crosslinker in prepolymer, which was prepared from a reaction of MDI and PCL-diol. The reinforcing effect of MWCNT in crosslinked MWCNT–PU nanocomposites was more pronounced as compared to that in conventional MWCNT–PU nanocomposites. MWCNT-crosslinked polyurethane containing 4 wt% modified MWCNTs showed the highest modulus and tensile strength among the composites. The presence of functionalized MWCNTs in the polymeric nanocomposite yielded enhancement in the thermal stability due to crosslinking of the MWCNTs with PU.

Soluble CNTs were prepared by treating SWCNTs with *sec*-butyl lithium and subsequently using the generated carbanions as the initiator to graft PtBA and PtBA-*b*-PMMA onto the surface of SWCNTs [104]. The anionic polymerization initiated by SWCNTs bearing carbanions not only provides a powerful strategy for functionalization of SWCNTs but also gives knowledge of the sidewall chemistry of SWCNTs. Liu et al. have performed functionalization onto CNT through the addition reaction between the initiators of ATRP and CNTs [105]. The modified CNTs were then served as an ATRP macro initiator for further modification. Both linear PS and V-shaped poly(styrene-*b*-*N*-isopropylacrylamide) block copolymers were therefore covalently bound to the CNT surface. The functionalized CNTs exhibited good solubility in organic solvents. In addition, amphiphilic and temperature-responsive behavior was observed with the CNTs functionalized with poly(styrene-*b*-*N*-isopropylacrylamide). A fascinating nano-object, amphiphilic polymer brushes with a hard core of MWCNTs and a relatively soft shell of polystyrene-*block*-poly(*N*-isopropylacrylamide) (PS-*b*-PNIPAm), was easily constructed by in situ RAFT polymerization of styrene followed by *N*-isopropylacrylamide on the modified convex surfaces of MWCNTs (MWCNT-PS) [106]. The MWCNT-PS-*b*-PNIPAm

had a PNIPAm block, which is very sensitive to temperature. Such a complex nano-object could open a door to the fabrication of novel functional carbon nanotube-based nanomaterials or nanodevices with designable structures and tailor-made properties.

The synergistic effect of using polystyrene-grafted MWCNT (PS-g-MWCNT) and a surfactant in the dispersion of MWCNT in a self-assembled poly(styrene-*b*-isoprene-*b*-styrene) (SIS) block copolymer was studied by Garate et al. [108]. The functionalization of MWCNT with polystyrene achieved by the “grafting from” approach is not enough to disperse them in the SIS block copolymer. However, a high dispersion of PS-g-MWCNT in SIS was achieved when dodecanethiol (DT) was added through composite preparation, without affecting the SIS capacity to self-assemble in ordered cylinders. Suspensions of PS-g-MWCNT without DT and non functionalized MWCNT with DT presented low stability forming aggregates in less than 10 min. On the contrary, the stability of PS-g-MWCNT suspension in the presence of DT was dramatically enhanced to more than 2 weeks. SWCNT-induced lyotropic phase behavior of a poly(ethylene glycol)-block-poly(propylene glycol)-block-poly(ethylene glycol) (F108) block copolymer/water system was also discussed [109]. As the concentration is increased by evaporation, the F108-SWCNT/water system exhibits isotropic hexagonal–face-centered cubic (FCC) and body-centered cubic (BCC)–lamellar transitions. This is in clear contrast with the F108/water system (isotropic–BCC–lamellar transitions), indicating that the hexagonal and the FCC phases are newly induced by the presence of one-dimensional SWCNTs. The SWCNTs maintain their individuality or very small bundle state in all phases except the lamellar phase. In the hexagonal phase, the SWCNTs were located in the hydrophobic core of F108 cylinders oriented parallel to the [001] direction. In the lamellar phase, the SWCNTs exist most likely in the hydrophobic layers forming aggregations among them.

Poly(lactide-co-caprolactone)-functionalized multiwalled carbon nanotubes (MWCNT-OH-g-PCLA)s were synthesized by in situ ROP of lactide (LA) and ϵ -caprolactone (CL) using stannous octanoate and hydroxylated MWCNTs (MWCNT-OHs) as the initiating system. The pristine MWCNTs were modified to possess carboxyl groups and then hydroxyl groups [110]. MWCNT-OHs are used as coiniciators to polymerize LA and CL by the surface-initiated ROP. The TGA analysis indicates that about 75 wt% of functionalized MWCNTs with PCLA belongs to grafted PCLA and the remaining 25 wt% to the initial MWCNT-OH.

Although progress in the use of CNT in medicine has been most encouraging for therapeutic and diagnostic applications, any translational success must involve overcoming the toxicology and surface functionalization challenges inherent in the use of such nanotubes. CNTs coated with a biocompatible block-copolymer composed of poly(lactide)-poly(ethylene glycol) (PLA-PEG) are reported to reduce short-term and long-term toxicity, sustain drug release of paclitaxel, and prevent aggregation [111]. The copolymer coating on the surface of CNTs significantly reduces in vitro toxicity. Moreover, the coating reduces the in vitro inflammatory response. Compared to non-coated CNTs, in vivo studies show no long-term inflammatory response with CNT coated with PLA-PEG and the surface coating significantly decreases acute toxicity by doubling the maximum tolerated dose in mice. Polystyrene-*b*-polyisoprene-*b*-polystyrene, a widely used linear triblock copolymer of the glassy-rubbery

glassy type, was used for the development of novel polymer nanocomposite materials [112]. Hybrid nanoadditives were prepared by the catalytic chemical vapor deposition method through which carbon nanotubes were grown on the surface of smectite clay nanolayers. Side-wall chemical organo functionalization of the nanotubes was performed in order to enhance the chemical compatibilization of the clay–CNT hybrid nanoadditives with the hydrophobic triblock copolymer. The hybrid clay–CNT nanoadditives were incorporated in the copolymer matrix by a simple solution mixing method. The prepared nanocomposites exhibited the enhanced mechanical properties compared to the pristine polymer and the nanocomposites prepared by conventional organo-clays.

2.2.2.2.2 FUNCTIONALIZATION OF GRAPHENE USING BLOCK COPOLYMERS

This section is focused on combining the extraordinary performances of GOSs with the multifunctional properties of block copolymers, and thus is useful to prepare a variety of composite materials. V-shaped copolymer brushes were grafted onto the surface of GO via coupling reactions [113]. Mid-block-functionalized ABC triblock copolymers with a short central B block were synthesized via the RAFT process using polyethylene glycol methyl ether 4-cyano-4-thiobenzoylthiopentanoate as the chain-transfer agent, glycidyl methacrylate, acrylic acid, and 3-methacryloyloxypropylsilane as the mid-block monomers, and further used as well-defined V-shaped copolymers to graft onto GO by coupling reactions. The film wettability and surface morphology of the resulting GO–copolymer nanocomposites were tunable by control over some factors such as temperature, solvent, and amphiphilicity of the grafted chains.

For polymer elastomers, the addition of stiff filler frequently results in enhanced stiffness but reduced toughness and ductility. Inspired by biomimetic studies, Chen and Lu demonstrated a new method that can simultaneously improve strength and toughness while maintaining the good ductility of PU elastomers [114]. The functional groups such as hydroxyl and epoxide groups on GNs enable PU oligomer chains to be covalently bonded to GNs by sequentially reacting with diisocyanate and polyethylene glycol oligomer. Noncovalently bonded PU oligomer chains are formed by the π – π interaction between GNs and pyrene derivatives. The resulting HO–GNs exhibit a good dispersion capacity in organic solvents and the PU matrix, improving the load transfer and the particle mobility in GN–PU composites. Cho's group has prepared highly flexible, conductive, and shape memory polyurethane nanocomposites using a robust and fast process [101]. Functionalized graphene sheets were incorporated as crosslinkers in the prepolymer, prepared from a reaction of MDI and PCL-diol. The covalently bonded graphene sheets were homogeneously dispersed in the polymer matrix. In comparison to pristine polyurethane and CNT crosslinked polyurethane, the graphene-crosslinked polyurethane composite exhibited higher modulus and breaking stress, and exceptional elongation-at-break.

A novel conjugated block copolymer, poly(9,9-dioctylfluorene)-block-poly(3-hexylthiophene) and its nanocomposite containing graphene sheets were synthesized for enhancing optoelectronic performance [115]. Graphene sheets were in situ formed in the polymer matrix via a reduction of octadecylamine-functionalized graphite oxide, where the graphite

oxide came from acidification and exfoliation of graphite. The blue-green light-emitting poly(9,9-dioctylfluorene) block and red-orange light-emitting P3HT block exhibited a combined white electroluminescence when the composite materials were fabricated as the emitting layer of a polymeric light-emitting diode. An efficient temperature-sensing platform was demonstrated using temperature-responsive, fluorescent Poly(7-(4-(acryloyloxy)butoxy)) coumarin-block-poly(*N*-isopropylacrylamide)-block-poly(styrene)azide (P7AC-*b*-PNIPAM-*b*-PSN₃) block copolymer-anchored graphene oxide sheets (FGO). FGO exhibited extraordinary stability in water and showed fast optical on–off switching behavior in response to temperature change [116].

The confinement of FGS in the PS domains of a nanostructured SIS block copolymer was reported [117]. The addition of FGS had a drastic effect on the nanostructured morphology of the block copolymer switching from long-range order cylinders of neat block copolymer to cylinders parallel and perpendicular to the free surface in the nanocomposite. The preparation of graphene/polymer composites by direct exfoliation of graphene from micro-sized graphite using a pyrene functionalized amphiphilic block copolymer, poly(pyrenemethyl acrylate)-*b*-poly[(polyethylene glycol) acrylate], in either aqueous or organic media was reported [118]. The composites were used to prepare sheets that exhibited increased tensile strength, compared to pure graphene and tunable conductivity. Jiang et al. demonstrated that graphene sheets could serve as a desirable inorganic constituent in constructing hybrid polymeric hydrogels via supramolecular routes [119]. GO nanosheets were modified by grafting β -cyclodextrins first, leading to chemical converted graphene (CCG), and then non-covalently functionalized by block copolymers, poly(*N,N*-dimethylacrylamide)-block-poly(*N*-isopropylacrylamide) (AZO-PDMA-*b*-PNIPAm) via inclusion complexation. Due to the thermo-sensitivity of the PNIPAm block, hybrid graphene inclusion complex solution exhibited sol–gel transition at elevated temperature. It was also found that the gelation temperature increased with the ratio of degree of polymerization of the PDMA block to the PNIPAm block of HGIC superstructures. The flexible and ultrathin 2-D planar structure of graphene sheets exhibited unprecedented advantage in constructing the 3-D network structure of the hydrogels, showing rapid sol–gel transition at elevated temperature.

2.2.2.3 Functionalization of CNTs and Graphene Using Dendritic Polymers

Dendritic polymers, such as dendrimeric and hyperbranched polymers, have generated great excitement in polymer research, owing to their wide range of applications from drug delivery to chemical sensors [120,121]. Taking advantage of their highly functionalized three-dimensional globular and nonentangled structures, the dendritic polymers have been used to enhance the dispersion of CNTs and graphene in polymer matrices. Here, this section is focused on the enhancement of CNTs and graphene dispersion due to their covalent functionalization with dendritic structures.

2.2.2.3.1 FUNCTIONALIZATION OF CNTS USING DENDRITIC POLYMERS

By surface modification with dendrimers or hyperbranched polymers, the solubility of CNTs can be improved greatly. Linear and hyperbranched glycopolymers, a kind of sugar-containing

polymers, were grown successfully from surfaces of MWCNTs by the “grafting from” strategy with good controllability and high reproducibility [122]. In both cases, a linear dependence of molecular weight on conversion was obtained, and the grafted polymer amount on MWCNTs was well controlled in a wide range by the reaction time and monomer conversion. In another study, carboxylic acid-terminated hyperbranched poly(ether-ketone) (HPEKs) were successfully grafted onto the surfaces of SWCNTs and MWCNTs to afford HPEK-g-SWCNT and HPEK-g-MWCNT nanocomposites [123]. The hyperbranched polymers were prepared via in situ polymerization of 5-phenoxyisophthalic acid as an AB₂ monomer for the HPEK in the presence of SWCNTs or MWCNTs in polyphosphoric acid/phosphorous pentoxide medium. The resultant nanocomposites were homogeneously dispersed in various common polar aprotic solvents.

Core-shell nanostructures with MWCNTs as the hard core and hyperbranched poly(urea-urethane) (HPU) trees as the soft shell were prepared by Yang et al. [124]. HPUs were covalently grafted onto the surfaces of MWCNTs terminated with multihydroxyl groups by a “grafting from” technique using one-pot polycondensation of diethanolamine and tolylene 2,4-diisocyanate. The grafted-HPU thickness on MWCNTs could be well controlled by adjusting the feed ratio of tolylene 2,4-diisocyanate to diethanolamine. The authors found that a large number of proton donor and proton acceptor groups were located in the HPU-functionalized MWCNTs; intra- and intermolecular H-bonds were easily formed by their interactions. At low temperature, shearing forces induced the conversion from intra- to intermolecular H-bonds. At high temperature, H-bonds in the HPU-functionalized MWCNTs were destroyed, and the packed structures of HPU trees became more loose.

Fluorinated dendrimer-type block copolymers were applied to the dispersion of SWCNTs and SWCNTs containing carboxy groups (SWCNT-COOH) in water [125]. Fluorinated block copolymer could disperse SWCNTs more effectively in water, compared to that of the corresponding ABA triblock-type fluoroalkyl end-capped di-methyl acrylamide oligomer (RF-(DMAA) n-RF). Interestingly, it was demonstrated that SWCNTs could be in part released from the fluorinated copolymeric aggregates/SWCNT composites or encapsulated into these composites with increasing dispersion times. On the other hand, fluorinated block copolymer and RF-(DMAA) n-RF oligomer were not able to disperse well (SWCNT)-COOH in water; however, ABA triblock-type fluoroalkyl end-capped acrylic acid oligomer was able to disperse quite effectively (SWCNT)-COOH in water. Well-dispersed epoxy/SWCNT composites were prepared by oxidization and functionalization of the SWCNT surfaces using polyamidoamine generation-0 dendrimer [126]. It was found that surface functionalization can effectively improve the dispersion and adhesion of SWCNTs in epoxy. This leads to enhancement in mechanical properties of epoxy, but the improvement is not as significant as expected. Prato et al. described the coupling between CNTs and a second-generation cyanophenyl-based dendrimer [127]. Using this approach, the attachment of dendrimers with a high density of functional groups onto the CNTs was achieved. These groups serve as anchor points for further reactions. With this aim, the authors have carried out a primary modification on to CNTs by the use of 1,3 dipolar cycloaddition reaction to obtained 238 and 511 mmol of pyrrolidine groups per gram, respectively. As a second step, dendrimer incorporation was

performed by carbodiimide chemistry. The attached dendrimer, with an estimated theoretical molecular length of 6.4 nm, generates a wrapping of 8 nm thick around the CNT walls.

The solvent-free MWCNT nanofluids were obtained through acid–base reaction and hydrogen bond roles with hyperbranched poly(amine-ester) (HPAE) [128]. The functionalized MWCNTs exhibited liquid-like behavior in the absence of solvent at room temperature. The functionalized MWCNTs are soluble in good solvent of HPAE, but insoluble in nonsolvent of HPAE. Their dispersibility, high thermal stability, and ability to flow at room temperature make them attractive as lubricants, plasticizers, and film-forming precursors. Polycondensation technique was applied for MWCNT functionalization by hyperbranched poly(urea-urethane)s (HPUs). MWCNT-HPU-filled polyamide-6 (PA6) nanocomposites were prepared by melt compounding [129]. MWCNT-HPUs were observed to disperse uniformly in the PA6 matrix, because the grafting of HPUs improved the compatibility between MWCNT-HPUs and PA6. The improved dispersion of MWCNT-HPUs in PA6 resulted in more efficient load transfer from polymer to MWCNTs. In addition, because of the hydrogen bond between hydroxyl groups on the surface of MWCNT-HPUs and carbonyl groups on the PA6 chains, the interfacial adhesion of PA6 and MWCNTs was further improved. Compared with PA6/MWCNT nanocomposite, PA6/MWCNT-HPU nanocomposite had lower crystallization temperature, faster crystallization rate, and higher crystallization degree.

Multiresponsive CNT gel was prepared via an ultrasound-induced assembly method. Hyperbranched polyamidoamine was grown from the surface of MWCNTs via a multistep Michael addition reaction, to link amido and amine units onto the surface [130]. These amido and amine units facilitate the assembly of MWCNTs with other functional polymers via hydrogen bonding, under ultrasound stimulus, to form a smart gel. The gelation is fast and controlled by ultrasound radiation strength, and the gels are responsive to mechanical stimuli such as vigorous agitation and to chemical stimuli such as water and acids. The MWCNTs were homogeneously embedded in the gel network, and the sol–gel switching was easily realized via heating and ultrasonication. Tetsuya et al. first reported the effects of generation 5 polyamidoamine dendrimer-functionalized fluorescent MWCNTs (dMWCNTs) on a mouse embryonic stem cell line [131]. The dendrimer-functionalized fluorescent MWCNTs were successfully synthesized, and could enter into embryonic stem cells quickly. The prepared dMWCNTs may be a highly efficient gene delivery system for ES cells, and have potential applications in ES research.

A facile approach to modify CNTs with multifunctional poly(amidoamine) (PAMAM) dendrimers for cancer cell targeting and imaging has been presented [132]. In this approach, fluorescein isothiocyanate (FI)- and folic acid (FA)-modified amine-terminated generation 5 (G5) PAMAM dendrimers were covalently linked to acid-treated MWCNTs, followed by acetylation of the remaining primary amine groups of the dendrimers. The resulting functionalized MWCNTs were water-dispersible, stable, and biocompatible. *In vitro* flow cytometry and confocal microscopy data show that the formed MWCNT composites can specifically target cancer cells over-expressing high-affinity folic acid receptors.

Zhu et al. demonstrated a new impedimetric DNA biosensor with second-generation poly(amidoamine) dendrimer (G2-PAMAM) covalently functionalized onto purified MWCNTs

and the as-formed G2-PAMAM-functionalized MWCNT composite (i.e., G2-PAMAM/MWCNT) was used both as the support to confine the single-stranded DNA (ssDNA) probe and as the electronic transducer to form the DNA biosensors [133]. The use of G2-PAMAM dendrimer attached onto an MWCNT electronic transducer as the tether for probe DNA provides a large number of amino groups to increase the surface binding of probe DNA, resulting in increasing the sensitivity of the impedimetric biosensor for the target DNA. The nanohybrids composed of silver nanoparticles and aromatic polyamide functionalized MWCNTs were successfully synthesized and tested for their antibacterial activity against different pathogens [134]. Prior to deposition of silver nanoparticles, acid-treated MWCNTs (MWCNT-COOH) were successively reacted with p-phenylenediamine and methylmethacrylate to form a series of NH₂-terminated aromatic polyamide dendrimers on the surface of MWCNTs through Michael addition and amidation. The existence of a high abundance of amine groups on the surface of functionalized MWCNTs (f-MWCNTs) provided sites for the formation of silver nanoparticles by the reduction of aqueous solution of AgNO₃. The silver nanoparticles formed in the resultant f-MWCNT–Ag nanohybrids were detected to be face-centered cubic symmetry. The antimicrobial activity of f-MWCNT–Ag nanohybrids were estimated against *E. coli*, *P. aeruginosa*, and *S. aureus* and compared with MWCNT-COOH and f-MWCNTs.

Hyperbranched polyurethane (HBPU) nanocomposites with MWCNTs were prepared by in situ polymerization on the basis of PCL-diol as the soft segment, MDI as the hard segment, and castor oil as the multifunctional group for the hyperbranched structure [135]. A dominant improvement in the dispersion of MWCNTs in the HBPU matrix was found and good solubility of HBPU–MWCNT nanocomposites in organic solvents was shown (Fig. 2-6).

To endow hydrophobic poly(vinylidene fluoride) (PVDF) membranes with reliable hydrophilicity and protein resistance, HPAE-functionalized MWCNTs were prepared to develop MWCNT-HPAE/PVDF nanocomposite membrane [136]. The results showed that MWCNT-HPAE was randomly dispersed at the individual nanotube levels in the membrane without obvious agglomerations. The hydrophilicity of nanocomposite membrane was enhanced due to the surface coverage of hydrophilic HPAE groups. Consequently, protein adsorption was significantly inhibited due to the hydrogen bonding interactions between hydrophilic groups

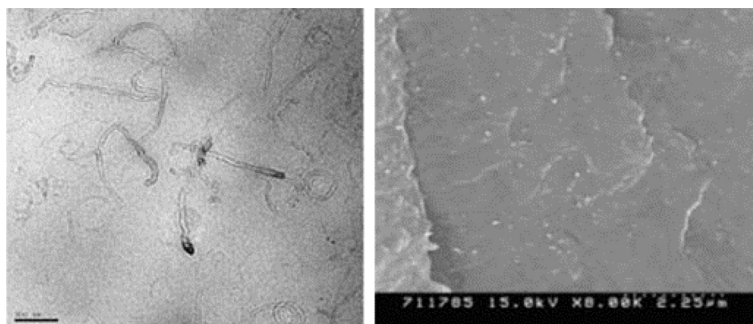


FIGURE 2-6 Dispersion of MWCNTs using hyperbranched polymers [135].

and water molecules. In addition, high water transport was obtained by the dual effect of hydrophilic MWCNT-HPAE and the pore structure of the membrane.

2.2.2.3.2 FUNCTIONALIZATION OF GRAPHENE USING DENDRITIC POLYMERS

A selective organic functionalization of graphene bulk or graphene edges was achieved by Quintana et al. [137]. Graphene sheets were functionalized with a PAMAM dendron, finding that graphene can be efficiently functionalized all over the surface, or only at the edges, depending on the reactions used in the functionalization process (Fig. 2-7). Zhao et al. reported a strategy using a three-dimensional and bulky dendritic structure to functionalize graphene sheets [138]. The authors found that the treatment of the acylchlorinated graphene oxide with dendritic anilines can easily load dendritic wedges to graphene oxide sheets and simultaneously reduce graphene oxide to graphene. The afforded dendronized graphene products possess excellent dispersibility in a variety of solvents. The dispersity shows great dependence on the size of the dendritic structure, in which the larger dendritic substituents afford better dispersity. Surprisingly, dendronization with an appropriate size of dendritic structure does not hamper but can even greatly enhance the bulk electrical conducting capability.

Hyperbranched aromatic polyamide functionalized graphene sheets (GS–HBA) have been synthesized and characterized [139], and the resulting GS–HBA exhibits uniform dispersion in a thermoplastic polyurethane (TPU) matrix and strong adhesion with the matrix by hydrogen-bond coupling, which improved the load transfer efficiency from the matrix to the GSs. Thus, the GS–HBA–TPU composites possess excellent mechanical performance and high dielectric performance. In addition, the hyperbranched polymer chains allow construction of a large number of microcapacitors and suppress the leakage current by isolating

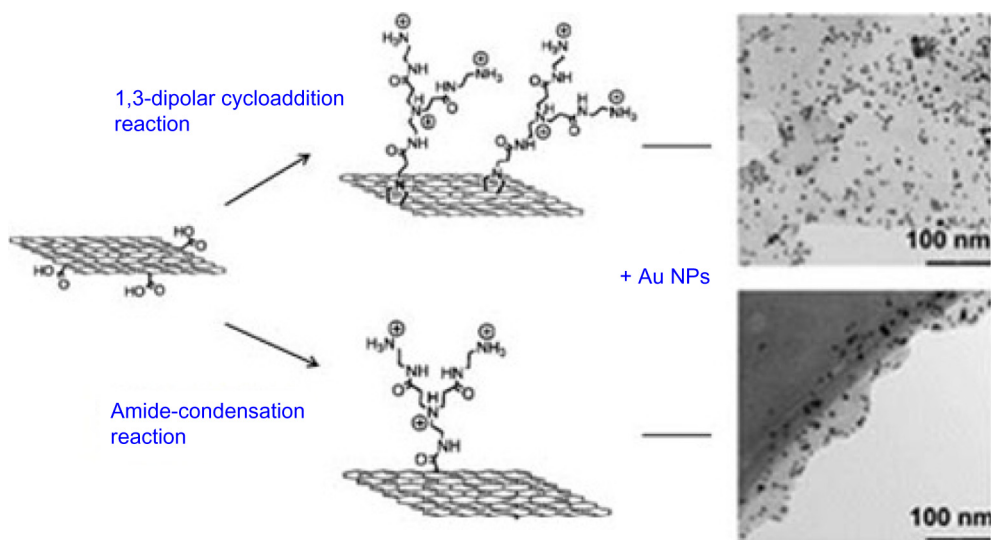


FIGURE 2-7 Selective organic functionalization of graphene edges [137].

the GSs in a TPU matrix, resulting in a higher permittivity and lower loss tangent for the GS–HBA composite in comparison with ethylene diamine-modified graphene, or hydrazine reduced-graphene composites.

A highly active catalyst based on PdCo alloy nanoparticles supported on polypropylenimine dendrimers, grown on graphene nanosheets, was synthesized and used for carbon–carbon cross-coupling Sonogashira reactions [140]. The prepared catalyst facilitated a facile, efficient, and environmentally friendly procedure for the Sonogashira reaction under copper- and solvent-free conditions using ultrasound irradiation at room temperature. The support of graphene showed that the catalyst could be easily recovered and reused several times without significant loss of activity. Graphene/gold nanoparticle multilayer films composed of polysodium 4-styrenesulfonate functionalized reduced graphene oxide and PAMAM dendrimer stabilized gold nanoparticles (AuNPs) were built up using the electrostatic layer-by-layer self-assembly technique on a glassy carbon electrode modified with a first layer of poly(diallyldimethylammonium chloride) [141]. Electrochemical studies exhibited that the layer-by-layer assembled RGO/AuNPs films possessed an excellent sensing performance for the detection of dopamine with a linear range from 1 to 60 mM and a limit of detection.

Graphene oxide was chemically functionalized using planar-structured first-generation polyamidoamine dendrimer (G1PAMAM) to form graphene core GG1PAMAM [142]. The monolayer of GG1PAMAM was anchored on the 3-mercapto propionic acid monolayer pre-immobilized onto a gold transducer. The GG1PAMAM was decorated using gold nanoparticles for the covalent attachment of single-stranded DNA through simple gold-thiol chemistry. The single- and double-stranded DNAs were discriminated electrochemically in the presence of redox probe $K_3[Fe(CN)_6]$. The use of linear and planar G1PAMAM along with the graphene core has enhanced the detection limit 100 times higher than the G1PAMAM with the conventional ethylene core. Hyperbranched polyglycerol with a bidentate aromatic segment in its focal point was synthesized and used to sandwich graphene sheets from the cut-edges [143]. Due to the hydrophobicity of the flat surface of the edge-functionalized graphenes and hydrophilicity of their edges, they changed their conformation from the extended to the closed state and formed nanocapsules in aqueous solution. Aqueous solution of nanocapsules and those with encapsulated doxorubicin were stable at room temperature for several weeks.

2.3 Conclusion

In this chapter, we have reviewed the surface modification of carbon nanomaterials (graphene and CNTs), processing methods, and mechanical and electrical properties and other applications of polymer/carbon nanomaterial-based nanocomposites. The surfaces of graphene and CNTs modify by noncovalent and covalent functionalization for improving the dispersion of these materials in polar solvents and interaction with polymer. The electrical, mechanical, and other properties of the composites were significantly enhanced by the addition of graphene and CNTs.

References

- [1] Kroto HW, Heath JR, O'Brien SC, Curl RF, Smalley RE. Buckminsterfullerene. *Nature* 1985;318:162.
- [2] Hirsch A. The chemistry of the fullerenes. *Anxewl Chem* 1994;107:1654.
- [3] Taylor R. The chemistry of fullerenes. *World Sci Singapore* 1995;4:288.
- [4] Hammond GS, Kuck VJ. Fullerenes: synthesis, properties and chemistry of large carbon clusters. *Am Chem Soc Washington, DC* 1992;481:161–75.
- [5] Hebard A. Buckminsterfullerene. *Ann Rev Mater Sci* 1993;23:159.
- [6] Iijima S. Helical microtubules of graphitic carbon. *Nature* 1991;354:56.
- [7] Harris PJF. Carbon nanotubes and related structures – new materials for the twenty-first century. *Cambridge: Cambridge University Express*; 2001.
- [8] Dresselhaus MS, Dresselhaus G, Eklund P. *Science of fullerenes and carbon nanotubes*. San Diego: Academic; 1996.
- [9] Dai L. *Carbon nanotechnology: recent developments in chemistry, physics, materials science and device applications*. London: Elsevier Science; 2006.
- [10] Dai L, Soundarrajan P, Kim T. Sensors and sensor arrays based on conjugated polymers and carbon nanotubes. *Pure Appl Chem* 2002;74:1753.
- [11] Dillon AC, Jones KM, Bekkedahl TA, Kiang CH, Bethune DS, Heben MJ. Storage of hydrogen in single-walled carbon nanotubes. *Nature* 1997;386:377.
- [12] Loh K, Kim J, Lynch J, Fangopol DM. In bridge maintenance, safety, management, health monitoring and informatics. *London: Taylor & Francis*; 2005.
- [13] Kumar A, Choudhury S, Saha S, Pahari S, De D, Bhattacharya S, et al. Thermoelectric power in ultrathin films, quantum wires and carbon nanotubes under classically large magnetic field: simplified theory and relative comparison. *Phys B Condens Matter* 2010;405:472–98.
- [14] Jin MHC, Dai L, Sun S, Cariciftci NS. In *organic photovoltaics: mechanisms, materials, and devices*. Boca Raton: CRC Press; 2005.
- [15] Liu Z, Lin X, Lee JY, Zhang W, Han M, Gan LM. Preparation and characterization of platinum-based electrocatalysts on multiwalled carbon nanotubes for proton exchange membrane fuel cells. *Langmuir* 2002;18:4054.
- [16] Yu D, Nagelli E, Du F, Dai L. Metal-free carbon nanomaterials become more active than metal catalysts and last longer. *J Phys Chem Lett* 2010;1:2165.
- [17] Welna DT, Qu L, Taylor BE, Dai L, Durstock MF. Vertically aligned carbon nanotube electrodes for lithium-ion batteries. *J Power Sources* 2010;196:1455.
- [18] Lu W, Qu L, Henry K, Dai L. High performance electrochemical capacitors from aligned carbon nanotube electrodes and ionic liquid electrolytes. *J Power Sources* 2009;189:1270–7.
- [19] Novoselov K, Geim A, Morozov S, Jiang D, Zhang Y, Dubonos S, et al. Electric field effect in atomically thin carbon films. *Science* 2004;306:666.
- [20] Enoki T, Takai K, Osipov V, Baidakova M, Vul A. Nanographene and nanodiamond; new members in the nanocarbon family. *Chem Asian J* 2009;4:796.
- [21] Liang J, Xu Y, Huang Y, Zhang L, Wang Y, Ma Y, et al. Infrared-triggered actuators from graphene-based nanocomposites. *J Phys Chem C* 2009;113:9921–7.
- [22] Wang X, Zhi L, Mullen K. Transparent, conductive graphene electrodes for dye-sensitized solar cells. *Nano Lett* 2008;8:323.
- [23] Yoo EJ, Kim J, Hosono E, Zhou H, Kudo T, Honma I. Large reversible Li storage of graphene nanosheet families for use in rechargeable lithium ion batteries. *Nano Lett* 2008;8:2277.

- [24] Vivekchand SRC, Rout CS, Subrahmanyam KS, Ovindaraj A, Rao CNR. Graphene-based electrochemical supercapacitors. *J Chem Sci* 2008;120:9.
- [25] Wang X, Zhi L, Tsao N, Tomovi Z, Li J, Mullen K. Transparent carbon films as electrodes in organic solar cells. *Angew Chem Int Ed* 2008;47:2990.
- [26] Eda G, Fanchini G, Chhowalla M. Large-area ultrathin films of reduced graphene oxide as a transparent and flexible electronic material. *Nat Nanotechnol* 2008;3:270.
- [27] Yang W, Ratinac KR, Ringer SP, Thordarson P, Gooding JJ, Brat F. Carbon nanomaterials in biosensors: should you use nanotubes or graphene? *Angew Chem Int Ed* 2010;49:2114.
- [28] Edwards DC. Polymer-filler interactions in rubber reinforcement. *J Mater Sci* 1990;25:4175–85.
- [29] Georgakilas V, Otyepka M, Bourlinos AB, Chandra V, Kim NK, Kemp C, et al. Covalent and non-covalent approaches, derivatives and applications. *Chem Rev* 2012;112:6156–214.
- [30] Liu J, Yang W, Tao L, Li D, Boyer C, Davis TP. Thermosensitive graphene nanocomposites formed using pyrene-terminal polymers made by RAFT polymerization. *J Polym Sci A Polym Chem* 2010;48:425–33.
- [31] Lomeda JR, Doyle CD, Kosynkin DV, Hwang WF, Tour JM. Diazonium functionalization of surfactant-wrapped chemically converted graphene sheets. *J Am Chem Soc* 2008;130:16201.
- [32] Xu YX, Bai H, Lu GW, Li C, Shi GQ. Flexible graphene films via the filtration of water soluble noncovalent functionalized graphene sheets. *J Am Chem Soc* 2008;130:5856.
- [33] Stankovich S, Dikin DA, Piner RD, Kohlhaas KA, Kleinhammes A, Jia Y, et al. Synthesis of graphene-based nanosheets via chemical reduction of exfoliated graphite oxide. *Carbon* 2007;45:1558.
- [34] Songlv Q, Cheng C, Mingjun C, Afang Z, Haichao Z, Liping W. Facile preparation of polyimide/graphene nanocomposites via an in situ polymerization approach. *RSC Adv* 2017;7:3003–11.
- [35] Sundeep D, Ephraim SD, Satish N. Use of nanotechnology in reduction of friction and wear. *IJIRAE* 2014;1:1–7.
- [36] Fei J, Luo W, Huang JF, Ouyang H, Xu Z, Yao C. Effect of carbon fiber content on the friction and wear performance of paper-based friction materials. *Tribol Int* 2015;87:91–7.
- [37] Mart Y, Guan JW, Lin SQ, Scriver C, Sturgeon RE, Simard B. Rapid and controllable covalent functionalization of single-walled carbon nanotubes at room temperature. *Chem Commun* 2007;5146–8.
- [38] Kocharova N, Aaritalo T, Leiro J, Kankare J, Lukkari J. Aqueous dispersion, surface thiolation, and direct self-assembly of carbon nanotubes on gold. *Langmuir* 2007;23:3363.
- [39] Antonello DC, Valeria E, Antonella F. Non-covalent and reversible functionalization of carbon nanotubes. *Beilstein J Nanotechnol* 2014;5:1675–90.
- [40] Xudong L, Raphae D, Step C, Anne SD, Christophe P, Christophe D, et al. Synthesis of pyrene-containing polymers and noncovalent sidewall functionalization of multiwalled carbon nanotubes. *Chem Mater* 2004;16:4005–11.
- [41] Yurekli K, Mitchell CA, Krishnamoorti R. Small angle neutron scattering from surfactant assisted aqueous dispersion of carbon nanotubes. *J Am Chem Soc* 2004;126:9902–3.
- [42] Jiang L, Gao L, Sun J. Production of aqueous colloidal dispersions of carbon nanotubes. *J Coll Interf Sci* 2003;260:89–94.
- [43] Poulin P, Vigolo B, Launois P. Films and fibers of oriented single wall nanotubes. *Carbon* 2002;40:1741–9.
- [44] Safar GAM, Ribeiro HB, Malard LM, Plentz FO, Fantini C, Santos AP. Optical study of porphyrin-doped carbon nanotubes. *Chem Phys Lett* 2008;462:109–11.
- [45] Tan Y, Resasco DE. Dispersion of single-walled carbon nanotubes of narrow diameter distribution. *J Phys Chem B* 2005;109:14454–60.

- [46] Sahoo NG, Rana S, Cho JW, Li L, Chan SH. Polymer nanocomposites based on functionalized carbon nanotubes. *Prog Polym Sci* 2010;35:837–67.
- [47] Islam MF, Rojas E, Bergey DM, Johnson AT, Yodh AG. High weight fraction surfactant solubilization of single-wall carbon nanotubes in water. *Nano Lett* 2003;3:269–73.
- [48] Sgobba V, Guldi DM. Carbon nanotubes as integrative materials for organic photovoltaic devices. *J Mater Chem* 2008;18:153–7.
- [49] Jakubka F, Schiel SP, Martin S, Englert JM, Hauke F, Hirsch A, et al. Effect of polymer molecular weight and solution parameters on selective dispersion of single-walled carbon nanotubes. *ACS Macro Lett* 2012;1:815–19.
- [50] Gwinner MC, Jakubka F, Gannott F, Siringhaus H, Zaumseil J. Enhanced ambipolar charge injection with semiconducting polymer/carbon nanotube thin films for light-emitting transistors. *ACS Nano* 2012;6:539–48.
- [51] Cui KM, Tria MC, Pernites R, Binag CA, Advincula RC. PVK/MWNT electrodeposited conjugated polymer network nanocomposite films. *ACS Appl Mater Interfaces* 2011;3:2300–8.
- [52] Rouse JH, Lillehei PT. Electrostatic assembly of polymer/single walled carbon nanotube multilayer films. *Nano Lett* 2003;3:59–62.
- [53] Wang S, Yu D, Dai L. Polyelectrolyte functionalized carbon nanotubes as efficient metal-free electrocatalysts for oxygen reduction. *J Am Chem Soc* 2011;133:5182–5.
- [54] Kolb HC, Finn MG, Sharpless KB. Click chemistry: diverse chemical function from a few good reactions. *Angew Chem Int Ed* 2001;40:2004–21.
- [55] Johnson JA, Finn MG, Koberstein JT, Turro NJ. Construction of linear polymers, dendrimers, networks, and other polymeric architectures by copper-catalyzed azide-alkyne cycloaddition “click” chemistry. *Macromol Rapid Commun* 2008;29:1052–72.
- [56] Li H, Cheng F, Duft AM, Adronov A. Functionalization of single-walled carbon nanotubes with well-defined polystyrene by “click” coupling. *J Am Chem Soc* 2005;127:14518–24.
- [57] Li H, Adronov A. Water-soluble SWCNTs from sulfonation of nanotube-bound polystyrene. *Carbon* 2007;45:984–90.
- [58] Rana S, Cho JW, Kumar I. Synthesis and characterization of polyurethane-grafted single-walled carbon nanotubes via click chemistry. *J Nanosci Nanotechnol* 2010;10:5700–7.
- [59] Yadav SK, Mahapatra SS, Cho JW. Synthesis of mechanically robust antimicrobial nanocomposites by click coupling of hyperbranched polyurethane and carbon nanotubes. *Polymer* 2012;53:2023–31.
- [60] Lee RS, Chen WH, Lin JH. Polymer-grafted multi-walled carbon nanotubes through surface-initiated ring-opening polymerization and click reaction. *Polymer* 2011;52:2180–8.
- [61] Yadav SK, Mahapatra SS, Cho JW, Lee JY. Functionalization of multiwalled carbon nanotubes with poly(styrene-*b*-(ethylene-co-butylene)-*b*-styrene) by click coupling. *J Phys Chem C* 2010;114:11395–400.
- [62] Battigelli A, Wang JTW, Russier J, Da Ros T, Kostarelos K, Al-Jamal KT, et al. Ammonium and guanidinium dendron–carbon nanotubes by amidation and click chemistry and their use for siRNA delivery. *Small* 2013;9:3610–19.
- [63] Lamanna G, Garofalo A, Popa G, Wilhelm C, Begin-Colin S, Felder-Flesch D, et al. Endowing carbon nanotubes with superparamagnetic properties: applications for cell labeling, MRI cell tracking and magnetic manipulations. *Nanoscale* 2013;5:4412–21.
- [64] Lee E, Park J, Im SG, Song C. Synthesis of single-walled carbon nanotube-incorporated polymer hydrogels via click chemistry. *Polym Chem* 2012;3:2451–5.
- [65] Moore E, Wang PY, Vogt AP, Gibson CT, Haridas V, Voelcker NH. Clicking dendritic peptides onto single walled carbon nanotubes. *RSC Adv* 2012;2:1289–91.

- [66] Rana S, Yoo HJ, Cho JW, Chun BC, Park JS. Functionalization of multi-walled carbon nanotubes with poly(ϵ -caprolactone) using click chemistry. *J Appl Polym Sci* 2011;2:1289–91.
- [67] Kumar I, Rana S, Rode CV, Cho JW. Functionalization of Single-Walled Carbon nanotubes with azides derived from amino acids using click chemistry. *J Nanosci Nanotechnol* 2008;8:3351–6.
- [68] Guo Z, Liang L, Liang JJ, Ma YF, Yang XY, Ren DM, et al. Covalently β -cyclodextrin modified single-walled carbon nanotubes: a novel artificial receptor synthesized by click chemistry. *J Nanopart Res* 2008;10:1077–83.
- [69] Georgakilas V, Gournis D, Tzitzios V, Pasquato L, Guldi DM, Prato M. Decorating carbon nanotubes with metal or semiconductor nanoparticles. *J Mater Chem* 2007;17:2679–94.
- [70] Wildgoose GG, Banks CE, Compton RG. Metal nanoparticles and related materials supported on carbon nanotubes: methods and applications. *Small* 2006;2:182–93.
- [71] Yadav S, Mahapatra S, Yoo H, Cho J. Synthesis of multi-walled carbon nanotube/polyhedral oligomeric silsesquioxane nanohybrid by utilizing click chemistry. *Nanoscale Res Lett* 2011;6:122.
- [72] Voggu R, Suguna P, Chandrasekaran S, Rao CNR. Assembling covalently linked nanocrystals and nanotubes through click chemistry. *Chem Phys Lett* 2007;443:118–21.
- [73] Islam MR, Bach LG, Nga TT, Lim KT. Covalent ligation of gold coated iron nanoparticles to the multi-walled carbon nanotubes employing click chemistry. *J Alloys Compd* 2013;561:201–5.
- [74] Yadav SK, Madeshwaran SR, Cho JW. Synthesis of a hybrid assembly composed of titanium dioxide nanoparticles and thin multi-walled carbon nanotubes using click chemistry. *J Colloid Interface Sci* 2011;358:471–6.
- [75] Rana S, Kumar I, Yoo HJ, Cho JW. Assembly of gold nanoparticles on single-walled carbon nanotubes by using click chemistry. *J Nanosci Nanotechnol* 2009;9:3261–3.
- [76] Jing L, Liang C, Shi X, Ye S, Xian Y. Fluorescent probe for Fe(III) based on pyrene grafted multiwalled carbon nanotubes by click reaction. *Analyst* 2012;137:1718–22.
- [77] Rana S, Cho JW. Core–shell morphology and characterization of carbon nanotube nanowires click coupled with polypyrrole. *Nanotechnology* 2011;22 275609.
- [78] Campidelli SP, Ballesteros B, Filoramo A, Diáz DDA, Torre GGDL, Torres TS, et al. Facile decoration of functionalized single-wall carbon nanotubes with phthalocyanines via click chemistry. *J Am Chem Soc* 2008;130:11503–9.
- [79] Palacin T, Khanh HL, Jousset B, Jegou P, Filoramo A, Ehli C, et al. Efficient functionalization of carbon nanotubes with porphyrin dendrons via click chemistry. *J Am Chem Soc* 2009;131:15394–402.
- [80] Sun S, Cao Y, Feng J, Wu P. Click chemistry as a route for the immobilization of well-defined polystyrene onto graphene sheets. *J Mater Chem* 2010;20:5605–7.
- [81] Cao Y, Lai Z, Feng J, Wu P. Graphene oxide sheets covalently functionalized with block copolymers via click chemistry as reinforcing fillers. *J Mater Chem* 2011;21:9271–8.
- [82] Ye YS, Chen YN, Wang JS, Rick J, Huang YJ, Chang FC, et al. Versatile grafting approaches to functionalizing individually dispersed graphene nanosheets using RAFT polymerization and click chemistry. *Chem Mater* 2012;24:2987–97.
- [83] Yadav SK, Yoo HJ, Cho JW. Click coupled graphene for fabrication of high-performance polymer nanocomposites. *Polym Sci B Polym Phys* 2012;51:39–47.
- [84] Jing Y, Tang H, Yu G, Wu P. Chemical modification of graphene with a thermotropic liquid crystalline polymer and its reinforcement effect in the polymer matrix. *Polym Chem* 2013;4:2598–607.
- [85] Castelaín M, Martínez G, Marco C, Ellis G, Salavagione HJ. Effect of click-chemistry approaches for graphene modification on the electrical, thermal, and mechanical properties of polyethylene/graphene nanocomposites. *Macromolecules* 2013;46:8980–7.

- [86] Liang J, Huang Y, Zhang L, Wang Y, Ma Y, Guo T, et al. Molecular-level dispersion of graphene into poly(vinyl alcohol) and effective reinforcement of their nanocomposites. *Adv Funct Mater* 2009;19:2297–302.
- [87] Wang Z, Ge Z, Zheng X, Chen N, Peng C, Fan C, et al. Polyvalent DNA-graphene nanosheets “click” conjugates. *Nanoscale* 2012;4:394–9.
- [88] Ragoussi ME, Casado S, Ribeiro-Viana R, Torre GDL, Rojo J, Torres T. Selective carbohydrate-lectin interactions in covalent graphene- and SWCNT-based molecular recognition systems. *Chem Sci* 2013;4:4035–41.
- [89] Zhou L, Shen Q, Zhao P, Xiang B, Nie Z, Huang Y, et al. Fluorescent detection of copper(II) based on DNA-templated click chemistry and graphene oxide. *Methods* 2013;64:299–304.
- [90] Yang H, Kwon Y, Kwon T, Lee H, Kim BJ. ‘Click’ preparation of CuPt nanorod-anchored graphene oxide as a catalyst in water. *Small* 2012;8:3161–8.
- [91] Wang HX, Zhou KG, Xie YL, Zeng J, Chai NN, Li J, et al. Photoactive graphene sheets prepared by “click” chemistry. *Chem Commun* 2011;47:5747–9.
- [92] Castelaín M, Salavagione H, Segura JL. “Click”-functionalization of [60]fullerene and graphene with an unsymmetrically functionalized diketopyrrolopyrrole (DPP) derivative. *Org Lett* 2012;14:2798–801.
- [93] Meng D, Sun J, Jiang S, Zeng Y, Li Y, Yan S, et al. Grafting P3HT brushes on GO sheets: distinctive properties of the GO/P3HT composites due to different grafting approaches. *J Mater Chem* 2012;22:21583–91.
- [94] Pan Y, Bao H, Sahoo NG, Wu T, Li L. Water-soluble poly(N-isopropylacrylamide)–Graphene sheets synthesized via click chemistry for drug delivery. *Adv Funct Mater* 2011;21:2754–63.
- [95] Yang Y, Song X, Yuan L, Li M, Liu J, Ji R, et al. Synthesis of PNIPAM polymer brushes on reduced graphene oxide based on click chemistry and RAFT polymerization. *J. Polym Sci A Polym Chem* 2012;50:329–37.
- [96] Yan H, Zhu L, Li X, Kwok A, Pan X, Zhao Y. A photoswitchable [2]rotaxane array on graphene oxide. *Asian J Org Chem* 2012;1:314–18.
- [97] Schnitzler T, Herrmann A. DNA block copolymers: functional materials for nanoscience and biomedicine. *Acc Chem Res* 2012;45:1419–30.
- [98] Priftis D, Sakellariou G, Mays JW, Hadjichristidis N. Novel diblock copolymer-grafted multiwalled carbon nanotubes via a combination of living and controlled/living surface polymerizations. *J Polym Sci A Polym Chem* 2010;48:1104–12.
- [99] Liu Y, Yao Z, Adronov A. Functionalization of single-walled carbon nanotubes with well-defined polymers by radical coupling. *Macromolecules* 2005;38:1172–9.
- [100] Yun S, Im H, Kim J. The effect of different hard segments in polyurethane on the electrical conductivity of polyurethane grafted multi-walled carbon nanotube/polyurethane nanocomposites. *Synth Met* 2011;161:1361–7.
- [101] Rana S, Cho JW, Tan LP. Graphene-crosslinked polyurethane block copolymer nanocomposites with enhanced mechanical, electrical, and shape memory properties. *RSC Adv* 2013;3:13796–803.
- [102] Meuer S, Braun L, Zentel R. Pyrene containing polymers for the non-covalent functionalization of carbon nanotubes. *Macromol Chem Phys* 2009;210:1528–35.
- [103] Jung YC, Sahoo NG, Cho JW. Polymeric nanocomposites of polyurethane block copolymers and functionalized multi-walled carbon nanotubes as crosslinkers. *Macromol Rapid Commun* 2006;27:126–31.
- [104] Chen S, Chen D, Wu G. Grafting of poly(tBA) and PtBA-b-PMMA onto the surface of SWNTs using carbanions as the initiator. *Macromol Rapid Commun* 2006;27:882–7.
- [105] Liu YL, Chen WH. Modification of multiwall carbon nanotubes with initiators and macroinitiators of atom transfer radical polymerization. *Macromolecules* 2007;40:8881–6.

- [106] Guoyong X, Wei-Tai W, Yusong W, Wenmin P, Qingren Z, Pinghua W. Functionalized carbon nanotubes with polystyrene- block -poly (N -isopropylacrylamide) by in situ RAFT polymerization. *Nanotechnology* 2007;18 145606.
- [107] Liu J, Nie Z, Gao Y, Adronov A, Li H. “Click” coupling between alkyne-decorated multiwalled carbon nanotubes and reactive PDMA-PNIPAM micelles. *J Polym Sci A Polym Chem* 2008;46:7187–99.
- [108] Garate H, Fascio ML, Mondragon I, D’Accorso NB, Goyanes S. Surfactant-aided dispersion of polystyrene-functionalized carbon nanotubes in a nanostructured poly(styrene-*b*-isoprene-*b*-styrene) block copolymer. *Polymer* 2011;52:2214–20.
- [109] Jang HS, Do C, Kim TH, Choi SM. Single-walled carbon nanotube-induced lyotropic phase behavior of a polymeric system. *Macromolecules* 2012;45:986–92.
- [110] Chakoli AN, Wan J, Feng JT, Amirian M, Sui JH, Cai W. Functionalization of multiwalled carbon nanotubes for reinforcing of poly(l-lactide-co- ϵ -caprolactone) biodegradable copolymers. *Appl Surf Sci* 2009;256:170–7.
- [111] Moore TL, Pitzer JE, Podila R, Wang X, Lewis RL, Grimes SW, et al. Multifunctional polymer-coated carbon nanotubes for safe drug delivery. *Part Part Syst Char* 2013;30:365–73.
- [112] Enotiadis A, Litina K, Gournis D, Rangou S, Avgeropoulos A, Xidas P, et al. Nanocomposites of polystyrene-*b*-poly(isoprene)-*b*-polystyrene triblock copolymer with clay “carbon nanotube hybrid nanoadditives. *J Phys Chem B* 2013;117:907–15.
- [113] Zhang P, Jiang K, Ye C, Zhao Y. Facile synthesis of V-shaped copolymer brushes grafted onto the surface of graphene oxide via coupling reactions. *Chem Commun* 2011;47:9504–6.
- [114] Chen Z, Lu H. Constructing sacrificial bonds and hidden lengths for ductile graphene/polyurethane elastomers with improved strength and toughness. *J Mater Chem* 2012;22:12479–90.
- [115] Chiu PC, Su RYT, Yeh JY, Yeh CY, Tsiang RCC. Synthesis and optoelectronic properties of nanocomposites comprising of poly(9,9-dioctylfluorene)-block-poly(3-hexylthiophene) block copolymer and graphene nanosheets. *J Nanosci Nanotechnol* 2013;13:3910–19.
- [116] Yang H, Paek K, Kim BJ. Efficient temperature sensing platform based on fluorescent block copolymer-functionalized graphene oxide. *Nanoscale* 2013;5:5720–4.
- [117] Peponi L, Tercjak A, Verdejo R, Lopez-Manchado MA, Mondragon I, Kenny JM. Confinement of functionalized graphene sheets by triblock copolymers. *J Phys Chem C* 2009;113:17973–8.
- [118] Liu Z, Liu J, Cui L, Wang R, Luo X, Barrow CJ, et al. Preparation of graphene/polymer composites by direct exfoliation of graphite in functionalised block copolymer matrix. *Carbon* 2013;51:148–55.
- [119] Liu J, Chen G, Jiang M. Supramolecular hybrid hydrogels from noncovalently functionalized graphene with block copolymers. *Macromolecules* 2011;44:7682–91.
- [120] Tomalia DA, Baker H, Dewald J, Hall M, Kallos G, Martin S, et al. Dendritic macromolecules: synthesis of starburst dendrimers. *Macromolecules* 1986;19:2466–8.
- [121] Ishizu K, Tsubaki K, Mori A, Uchida S. Architecture of nanostructured polymers. *Prog Polym Sci* 2003;28:27–54.
- [122] Gao C, Muthukrishnan S, Li W, Yuan J, Xu Y, Müller AHE. Linear and hyperbranched glycopolymer-functionalized carbon nanotubes: synthesis, kinetics, and characterization. *Macromolecules* 2007;40:1803–15.
- [123] Choi JY, Han SW, Huh WS, Tan LS, Baek JB. In situ grafting of carboxylic acid-terminated hyperbranched poly(ether-ketone) to the surface of carbon nanotubes. *Polymer* 2007;48:4034–40.
- [124] Yang Y, Xie X, Yang Z, Wang X, Cui W, Yang J, et al. Controlled synthesis and novel solution rheology of hyperbranched poly(urea – urethane)-functionalized multiwalled carbon nanotubes. *Macromolecules* 2007;40:5858–67.

- [125] Sawada H, Naitoh N, Kasai R, Suzuki M. Dispersion of single-walled carbon nanotubes in water by the use of novel fluorinated dendrimer-type copolymers. *J Mater Sci* 2008;43:1080–6.
- [126] Sun L, Warren GL, O'Reilly JY, Everet WN, Lee SM, Davis D, et al. Mechanical properties of surface-functionalized SWCNT/epoxy composites. *Carbon* 2008;46:320–8.
- [127] García A, Herrero MA, Frein S, Deschenaux R, Muñoz R, Bustero I, et al. Synthesis of dendrimer–carbon nanotube conjugates. *Phys Status Solidi (a)* 2008;205:1402–7.
- [128] Zhang J, Zheng Y, Yu P, Mo S, Wang R. The synthesis of functionalized carbon nanotubes by hyper-branched poly(amine-ester) with liquid-like behavior at room temperature. *Polymer* 2009;50:2953–7.
- [129] Zhang RH, Yang YK, Xie XL, Li RKY. Dispersion and crystallization studies of hyper-branched poly(urea-urethane)s-grafted carbon nanotubes filled polyamide-6 nanocomposites. *Compos Pt A Appl Sci Manuf* 2010;41:670–7.
- [130] You YZ, Yan JJ, Yu ZQ, Cui MM, Hong CY, Qu BJ. Multi-responsive carbon nanotube gel prepared via ultrasound-induced assembly. *J Mater Chem* 2009;19:7656–60.
- [131] Cui D, Zhang H, Wang Z, Asahi T, Osaka T. Effects of dendrimer-functionalized multi-walled carbon nanotubes on murine embryonic stem cells. *ECS Trans* 2008;13:111–16.
- [132] Shi X, Wang SH, Shen M, Antwerp ME, Chen X, Li C, et al. Multifunctional dendrimer-modified multiwalled carbon nanotubes: synthesis, characterization, and in Vitro cancer cell targeting and imaging. *Biomacromolecules* 2009;10:1744–50.
- [133] Zhu N, Gao H, Xu Q, Lin Y, Su L, Mao L. Sensitive impedimetric DNA biosensor with poly(amidoamine) dendrimer covalently attached onto carbon nanotube electronic transducers as the tether for surface confinement of probe DNA. *Biosensor Bioelectron* 2010;25:1498–503.
- [134] Neelgund GM, Oki A. Deposition of silver nanoparticles on dendrimer functionalized multiwalled carbon nanotubes: synthesis, characterization and antimicrobial activity. *J Nanosci Nanotechnol* 2011;11:3621–9.
- [135] Sravendra R, Niranjana K, Jae WC, Young Ho K. Enhanced dispersion of carbon nanotubes in hyper-branched polyurethane and properties of nanocomposites. *Nanotechnology* 2008;19:495707.
- [136] Zhao X, Ma J, Wang Z, Wen G, Jiang J, Shi F, et al. Hyperbranched-polymer functionalized multi-walled carbon nanotubes for poly(vinylidene fluoride) membranes: From dispersion to blended fouling-control membrane. *Desalination* 2012;303:29–38.
- [137] Quintana M, Montellano A, del Rio Castillo AE, Tendeloo GV, Bittencourt C, Prato M. Selective organic functionalization of graphene bulk or graphene edges. *Chem Commun* 2011;47:9330–2.
- [138] Zhao FG, Li WS. Dendronized graphenes: remarkable dendrimer size effect on solvent dispersity and bulk electrical conductivity. *J Mater Chem* 2012;22:3082–7.
- [139] Wu C, Huang X, Wang G, Wu X, Yang K, Li S, et al. Hyperbranched-polymer functionalization of graphene sheets for enhanced mechanical and dielectric properties of polyurethane composites. *J Mater Chem* 2012;22:7010–19.
- [140] Shaabani A, Mahyari M. PdCo bimetallic nanoparticles supported on PPI-grafted graphene as an efficient catalyst for sonogashira reactions. *J Mater Chem A* 2013;1:9303–11.
- [141] Liu S, Yan J, He G, Zhong D, Chen J, Shi L, et al. Layer-by-layer assembled multilayer films of reduced graphene oxide/gold nanoparticles for the electrochemical detection of dopamine. *J Electroanal Chem* 2012;672:40–4.
- [142] Jayakumar K, Rajesh R, Dharuman V, Venkatesan R. Graphene-PAMAM dendrimer-gold nanoparticle composite for electrochemical DNA hybridization detection. *Methods Mol Biol* 2013;1039:201–19.
- [143] Movahedi S, Adeli M, Fard AK, Maleki M, Sadeghizadeh M, Bani F. Edge-functionalization of graphene by polyglycerol; A way to change its flat topology. *Polymer* 2013;54:2917–25.